Title	Involvement of thrombin and mitogen-activated protein kinase pathways in hemorrhagic brain injury
Author(s)	Ohnishi, Masatoshi; Katsuki, Hiroshi; Fujimoto, Shinji; Takagi, Mikako; Kume, Toshiaki; Akaike, Akinori
Citation	Experimental Neurology, 206(1): 43-52
Issue date	2007-07
Type	Journal Article
URL	http://hdl.handle.net/2298/10013
Right	© 2007 Elsevier Inc. All rights reserved.

Involvement of thrombin and mitogen-activated protein kinase pathways in hemorrhagic brain injury

Masatoshi Ohnishi, Hiroshi Katsuki, Shinji Fujimoto, Mikako Takagi, Toshiaki Kume, Akinori Akaike

Department of Pharmacology, Graduate School of Pharmaceutical Sciences, Kyoto University, 46-29 Yoshida-shimoadachi-cho, Sakyo-ku, Kyoto 606-8501, Japan.

Address correspondence to Akinori Akaike, Ph.D.

Department of Pharmacology,

Graduate School of Pharmaceutical Sciences, Kyoto University

46-29 Yoshida-shimoadachi-cho, Sakyo-ku, Kyoto 606-8501, Japan.

Phone: +81-75-753-4550 FAX: +81-75-753-4579

E-mail: aakaike@pharm.kyoto-u.ac.jp

Abstract

Thrombin is thought to play an important role in brain damage associated with intracerebral hemorrhage (ICH). We previously showed that activation of mitogen-activated protein (MAP) kinases and recruitment of microglia are crucial for thrombin-induced shrinkage of the striatal tissue in vitro and thrombin-induced striatal damage in vivo. Here we investigated whether the same mechanisms are involved in ICH-induced brain injury. A substantial loss of neurons was observed in the center and the peripheral region of hematoma at 3 days after ICH induced by intrastriatal injection of collagenase in adult rats. Intracerebroventricular injection of argatroban or cycloheximide, both of which prevent thrombin cytotoxicity in vitro, exhibited a significant neuroprotective effect against ICH-induced injury. ICH-induced neuron loss was also prevented by a MAP kinase kinase inhibitor (PD98059) and a c-Jun N-terminal kinase inhibitor (SP600125). These drugs had no effect on hematoma size or ICH-induced brain edema. Activation of extracelluar signal-regulated kinase in response to ICH was observed in both neurons and microglia. Despite their neuroprotective effects, MAP kinase inhibitors did not decrease the number of terminal deoxynucleotidyl transferase-mediated dUTP nick-end labeling (TUNEL)-positive cells appearing after ICH. Identification of cell types revealed that TUNEL staining occurred prominently in neurons but not in microglia, whereas inhibition of MAP kinases resulted in appearance of TUNEL staining in microglia. These results suggest that thrombin and the activation of MAP kinases are involved in ICH-induced neuronal injury, and that neuroprotective effects of MAP kinases are in part mediated by arrestment of microglial activities.

Keywords: intracerebral hemorrhage; microglia; thrombin; mitogen-activated protein kinase; apoptosis

Introduction

Intracerebral hemorrhage (ICH) is characterized by breakdown of blood vessels within the brain parenchyma, which triggers a substantial loss of neurons that frequently leads to poor prognosis (Fayad and Awad, 1998). Fundamental therapeutic strategies for ICH, particularly those aimed at neuroprotection, have yet to be established.

Blood-intrinsic factors are primarily involved in neuronal damage occurring after ICH. Several lines of evidence have indicated that thrombin, a blood coagulation factor, plays an important role in the pathogenesis of ICH, although other factors such as hemoglobin may also participate in neuron loss (Xi et al., 2006). At low concentrations, thrombin may provide cytoprotective effects on neurons and astrocytes against oxidative stress and ischemic injury (Donovan and Cunningham, 1998; Striggow et al., 2000; Vaughan et al., 1995). By contrast, uncontrolled thrombin activity after ICH may be involved in neuronal cell death as well as brain edema. Indeed, a thrombin inhibitor argatroban has been shown to suppress the progression of pathogenic events following ICH (Kitaoka et al., 2002; Nagatsuna et al., 2005). Thrombin, with its serine protease activity, stimulates G protein-coupled receptors designated as proteinase-activated receptors (PARs), which are widely distributed in the central nervous system (Flynn et al., 2004; Noobakhsh et al., 2003). Stimulation of PARs activates various intracellular signaling enzymes, including members of mitogen-activated protein (MAP) kinase family such as extracelluar signal-regulated kinase (ERK), p38 mitogen-activated protein kinase (p38 MAPK) and c-Jun N-terminal kinase (JNK) (Marinissen et al., 2003; Suo et al., 2003; Wang et al., 2002).

Recently, we investigated the mechanisms of thrombin-induced neuronal injury in vitro (Fujimoto et al., 2006) and in vivo (Fujimoto et al., 2007). In organotypic cortico-striatal slice cultures, thrombin induced shrinkage of the striatal tissue, which was prevented by inhibition of ERK, p38 MAPK or JNK. In addition, depletion of microglia protected striatal

tissue from thrombin-induced injury (Fujimoto et al., 2006). Activation of MAP kinase pathways and recruitment of microglia have also been demonstrated in neuronal injury induced by intrastriatal injection of thrombin in adult rats (Fujimoto et al., 2007).

Given that thrombin is involved in ICH-associated neuronal injury, one can assume that signaling mechanisms similar to those recruited by thrombin insults plays an important role in the pathogenesis of ICH. However, effects of MAP kinase inhibition on ICH-induced injury have not been reported. Therefore, in the present study we addressed this issue using an established animal model of ICH, i.e., rats that received intrastriatal microinjection of collagenase (Terai et al., 2003; Xue et al., 2003).

Materials and methods

Induction of intracerebral hemorrhage and drug treatment

Experiments were conducted in accordance with the ethical guidelines of Kyoto University animal experimentation committee, and with the Guidelines of the United States National Institutes of Health regarding the care and use of animals for experimental procedures. Drugs and chemicals were obtained from Nacalai Tesque (Kyoto, Japan), unless otherwise indicated.

We used 208 male Sprague-Dawley rats (Nihon SLC, Shizuoka, Japan) weighing 220 to 280 g. Animals were maintained at constant ambient temperature (22 ± 1 °C) under a 12 h light and dark cycle. After intraperitoneal injection of pentobarbital (50 mg/kg, Dainippon-Sumitomo, Osaka, Japan), rats were placed in a stereotaxic frame (Narishige, Tokyo, Japan). Each rat was implanted with stainless steel guide cannulas (o.d. 0.7 mm) above the right striatum (3 mm lateral to midline, 0.2 mm anterior to coronal suture of the bregma) and above the lateral ventricle (1.5 mm lateral to midline, 0.8 mm posterior to coronal suture of the bregma). Guide cannulas were held firmly in place by dental acrylic cement (Nissin Dental Products Inc., Kyoto, Japan). The 27-gauge injection cannula, whose tip was inserted 6.0 mm below the surface of the skull, was introduced through a guide cannula into the right striatum, and then ICH was induced by injection of 0.25 U collagenase type IV (Sigma, St. Louis, MO, USA) in 5 μl saline, at a constant rate of 0.50 μl/min with a microinfusion pump. Argatroban (2.5 μg, Sawai Pharmaceuticals, Osaka, Japan) and cycloheximide (10 nmol, Wako Pure Chemicals, Osaka, Japan) were injected into the ipsilateral ventricle 1 h before induction of ICH, and then once daily afterwards for 3 days. MAP kinase inhibitors (PD98059 (Calbiochem, San Diego, CA, USA), SB203580 (Calbiochem) and SP600125 (Tocris Cookson, Bristol, UK), 5 nmol respectively) with 33% DMSO as vehicle were injected into the contralateral ventricle at the same time course as that

for argatroban and cycloheximide. Each drug solution in a volume of 5 μl/rats was infused at a constant rate of 10.0 μl/min. In several sets of experiments where histological and biochemical determinations were done at less than 48 h after ICH, rats received injection of drugs only at 1 h before collagenase injection. After injection, the injection cannula was left in place for 5 min and then removed slowly. The scalp incision was sutured, and rats were placed in a cage with free access to food and water.

Immunohistochemistry and assessment of hematoma size

Three days or 8 h after ICH, rats were anesthetized again and perfused transcardially with 60 ml cold phosphate-buffered saline (PBS) followed by 60 ml of 4% paraformaldehyde (PFA). Brains were isolated and fixed in 4% PFA for 2 h and then were soaked in 15% sucrose overnight at 4 °C. After freezing, they were cut into sections of 16 μm thicknesses with a Cryostat (Leica Microsystems, Germany) and were pasted to silanized slide glasses. Activation of NeuN antigen was achieved by soaking of specimens in 10 mM citric acid (pH 6.0) for 15 min at 121 °C with autoclave. After rinse with PBS, specimens were treated with 0.5% Triton X-100 in PBS containing 1.5% horse or goat serum for 1 h at room temperature, then incubated with primary antibodies overnight at 4 °C. Primary antibodies were mouse anti-NeuN (1:200, Chemicon International, Temecula, CA, USA), mouse anti-OX-42 (1:300, Dainippon Pharmaceutical, Osaka, Japan) and rabbit anti-phospho-p44/42 MAP kinase (T202/204) (1:250, Cell Signaling Technology, Beverly, MA, USA). After rinse with PBS, specimens were incubated with corresponding secondary antibodies for 1 h at room temperature. Alexa Fluor 488-labeled goat anti-rabbit IgG (1:200, Molecular Probes, Eugene, OR, USA), Alexa Fluor 568-labeled goat anti-mouse IgG (1:200, Molecular Probes) and biotinylated anti-mouse IgG (1:200, Vector Laboratories, Burlingame, CA, USA) were used as secondary antibodies. After incubation with the biotinylated secondary antibody,

specimens were treated with avidin-biotinylated horseradish peroxidase complex (Vectastain Elite ABC kit, Vector Laboratories) and then peroxidase was visualized with diaminobendizine and H_2O_2. Bright-field images were captured through a monochrome chilled CCD camera (C5985; Hamamatsu Photonics, Hamamatsu, Japan) and stored as image files. The number of NeuN- or OX-42-positive cells per 230 × 320 μm^2 was counted at the center and the peripheral region of hematoma as shown in Fig. 1. The area with low NeuN-immunoreactivity in a coronal section containing a track of cannula for collagenase injection was taken as hematoma area, which was quantified with Scion image. Fluorescence signals were observed with a laser-scanning confocal microscopic system (MRC1024, Biorad, Hercules, CA, USA).

Measurement of brain water content

Three days after ICH, rats were decapitated under deep anesthesia. Two coronal brain slices (A and B) with 3 mm thickness were cut at 3 mm from the frontal pole. Slice A contained the bleeding site by collagenase injection, and slice B was adjacent and caudal to slice A. Slices were divided into the ipsilateral and the contralateral side and the wet weight of these samples were obtained. Samples were then dried in a gravity oven at 75 °C for 12 h to give the dry weight. The water content was calculated by the following formula: (wet weight – dry weight) / wet weight × 100 (%).

Western blot analysis

Rats were decapitated under deep anesthesia at 4, 8, 24 and 48 h following ICH. Rats of control group were decapitated at 4 h after intrastriatal injection of saline. The striatal tissue adjacent to the hematoma were homogenized in ice-cold lysis buffer consisting of 20 mM Tris-HCl (pH 7.0), 25 mM β-glycerophosphate (Sigma), 2 mM EGTA･2Na, 1% Triton X-100,

1 mM vanadate, 1% aprotinin (Sigma), 1 mM phenylmethylsulfonyl fluoride and 2 mM dithiothreitol. Samples were mixed with a sample buffer composed of 124 mM Tris-HCl (pH 6.8), 4% sodium dodecyl sulfate (SDS), 10% glycerol, 0.02% bromophenol blue and 4% 2-mercaptoethanol. After boiling for 5 min, samples were subjected to 12% SDS-polyacrylamide gel electrophoresis for 70 min, followed by transfer to PVDF membrane (Millipore) for 70 min. Membranes were blocked for at least 1 h by 5% nonfat milk at room temperature and subsequently incubated overnight with mouse anti-phospho-p44/42 MAP kinase (T202/Y204) (1:2000, Cell Signaling Technology) and anti-p-44/42 MAP kinase (1:1000, Cell Signaling Technology). The membranes were rinsed and incubated with horseradish peroxidase-conjugated goat anti-mouse IgG (1:10000, Jackson Immunoresearch Laboratories) and goat anti-rabbit IgG (1:10000, Jackson Immunoresearch Laboratories). After incubation with secondary antibodies, membranes were rinsed and bound antibodies were detected with enhanced chemiluminescence kit (Amersham Bioscience, Buckinghamshire, UK) according to the manufacturer's instructions. The band intensities were analyzed with Scion Image.

Terminal deoxynucleotidyl transferase-mediated dUTP nick-end labeling (TUNEL)

TUNEL was carried out with a commercial kit (TAKARA BIO Inc., Shiga, Japan). One day after ICH, rats were decapitated under deep anesthesia, brains were isolated and frozen, and coronal brain sections (16 μm) were prepared and mounted onto slides. Specimens were then fixed with 4% PFA for 15 min at room temperature. Epitope was retrieved by treatment with 20 μg/ml proteinase K (Ambion, USA) for 20 min at room temperature. Intrinsic peroxidase was blocked with 3% H_2O_2 applied for 10 min, and after permeabilization, specimens were incubated with constructed labeling reaction solution containing TdT enzyme (1:10) for 120 min at 37 °C. After rinse with PBS, specimens were incubated with

anti-FITC HRP conjugate as a primary antibody overnight at 37 °C, and then, with biotinylated anti-rabbit IgG (1:200) for 2 h at room temperature. After rinse with PBS, specimens were treated with avidin-biotinylated horseradish peroxidase complex. Peroxidase was visualized with diaminobendizine and H_2O_2, or with Tyramide Signal Amplification kit with Alexa Fluor 488 (Molecular Probes). Specimens with fluorescent TUNEL staining were further processed for immunohistochemistry. Mouse anti-NeuN (1:200) and mouse anti-OX-42 (1:300) were used as primary antibodies, and Alexa Fluor 568-labeled goat anti-mouse IgG (1:200) was used as a secondary antibody.

Statistics

Data are expressed as means ± SEM. Statistical significance of difference was evaluated with one-way analysis of variance followed by Student-Newman-Keuls' test, unless otherwise indicated. When the data sets were not suitable for these parametric tests, non-parametric Kruskal-Wallis test followed by Dunn's multiple comparisons test was used. Probability values less than 5% were considered significant.

Results

ICH-induced loss of striatal neurons is prevented by argatroban and cycloheximide

We injected collagenase into the right striatum of adult rats to evoke ICH. Brain sections were obtained 3 days after collagenase injection and immunostained with an antibody against NeuN, a neuronal marker. Macroscopic observations of immunostained sections revealed that the striatal region corresponding to the hematoma area of collagenase-injected rats exhibited much lower NeuN-positive signals, compared to the striatum of saline-injected rats (Fig. 1A and B). At higher magnification, a substantial decrease in the number of NeuN-positive cells was evident within the hematoma area (Fig. 1D, compared to Fig. 1C).

Argatroban, a thrombin inhibitor, has been shown to inhibit thrombin-induced injury of striatal tissue in organotypic slice culture (Fujimoto et al., 2006). To clarify the involvement of thrombin in ICH-induced injury, we examined the effect of repeated intracerebroventricular (i.c.v.) injection of argatroban. We used argatroban at the highest dose (2.5 μg) contained in an injection solution, which was the only formula of this drug commercially available. Treatment with 2.5 μg argatroban 1 h before, as well as 1 and 2 days after collagenase injection, significantly increased the number of remaining NeuN-positive cells at the hematoma center, i.e., around the injection site of collagenase (Fig. 2A-C, E). The number of surviving neurons was also increased in the peripheral region of hematoma by argatroban treatment, although the effect did not reach statistical significance (Fig. 2F).

Our previous study also demonstrated that cycloheximide, a protein synthesis inhibitor, prevented thrombin-induced striatal injury in vitro (Fujimoto et al., 2006). Consistent with this observation, treatment with 10 nmol cycloheximide, in the same manner as that with argatroban, significantly increased the number of surviving neurons in the hematoma center (Fig. 2D, E) and tended to increase the number of surviving neurons in the peripheral region of hematoma (Fig. 2F). A lower dose (1 nmol) of cyloheximide showed no effect (data not

shown). The extent of protection by 2.5 μg argatroban and 10 nmol cycloheximide did not differ significantly with each other.

ICH-induced loss of striatal neurons is prevented by MAP kinase inhibitors

Thrombin triggers activation of multiple members of MAP kinase family, including ERK, p38 MAPK and JNK (Flynn et al., 2004; Noobakhsh et al., 2003). All of these MAP kinases participate in thrombin-induced striatal tissue injury in culture (Fujimoto et al., 2006). Accordingly, we examined the effects of MAP kinase inhibitors against ICH-induced neuronal injury. We used PD98059 as an ERK kinase inhibitor, SB203580 as a p38 MAPK inhibitor and SP600125 as a JNK inhibitor. DMSO was used at 33% in a vehicle for i.c.v. injection of these inhibitors because of their poor solubility. As compared to saline, 33% DMSO produced no effect on the number of neurons (compare Fig. 3 with Fig. 2). In addition, i.c.v. injection of DMSO had no effect on brain water content (Fig. 4) and the number of TUNEL- and OX-42-positive cells (data not shown). Furthermore, we did not observe any abnormal behaviors in rats injected with 33% DMSO. The doses of inhibitors were set to 5 nmol, based on the fact that all of these drugs at 100 μM prevented thrombin-induced shrinkage of the striatal tissue in vitro (Fujimoto et al., 2006). Also, poor solubility of these drugs hampered their usage at higher doses. I.c.v. injections of PD98059 1 h before, as well as 1 and 2 days after collagenase injection, significantly increased the number of surviving neurons in the hematoma center and in the peripheral region of hematoma at 3 days after collagenase injection (Fig. 3). SP600125 applied in the same manner significantly increased the number of surviving neurons in the peripheral region of hematoma, and tended to increase the number of surviving neurons in the hematoma center. SB203580 also tended to increase the number of surviving neurons both in the hematoma center and in the peripheral region of hematoma, but the effect did not reach statistical significance. Overall, the protective effect

of PD98059 was most prominent in the sense that this drug was effective both in the center and the peripheral region of hematoma, although we did not obtain a statistically significant difference among the effects of PD98059, SB203580 and SP600125.

Argatroban, cycloheximide, and MAP kinase inhibitors do not affect hematoma size and brain water content

We next examined the effects of drugs on the size of hematoma, to determine if these drugs may affect the amount of bleeding after ICH. We regarded the striatal region with low NeuN immunoreactivity as the area invaded by hematoma, and measured the hematoma size 3 days after ICH, in the coronal section containing the track of cannula for collagenase injection. The size of hematoma in rats treated with argatroban and cyclohexmide was 10.7 ± 0.5 mm^2 ($n = 9$) and 9.9 ± 1.0 mm^2 ($n = 10$), respectively. These values were not significantly different from the value in control rats that received i.c.v. injections of saline (11.9 ± 0.9 mm^2, $n = 8$). Similarly, the size of hematoma in rats treated with PD98059 (11.1 ± 0.9 mm^2, $n = 7$), SB203580 (11.8 ± 1.1 mm^2, $n = 8$) or SP600125 (11.0 ± 0.4 mm^2, $n = 8$) was not different from that in rats treated with 33% DMSO as vehicle (10.8 ± 0.5 mm^2, $n = 8$).

ICH is associated with brain edema, which by itself may be deleterious to neuronal viability (Hua et al., 2002). Therefore, we measured brain water content 3 days after collagenase injection (Fig. 4). We observed a robust increase in water content in the tissue containing the site of collagenase injection (ipsilateral side of slice A), and to a lesser extent, in the adjacent tissue (ipsilateral side of slice B). Argatroban, cycloheximide, and MAP kinase inhibitors had no effect on the increase of brain water content. Overall, the results indicate that the neuroprotective effects of these drugs do not result from suppression of hematoma expansion or of edema formation.

ERK activation occurs in neurons and microglia after ICH

Of the MAP kinase inhibitors, PD98059 was most effective in preventing ICH-induced neuronal loss. Accordingly, we examined changes in the activation status of ERK in response to ICH. Western blotting of striatal tissue samples showed that ICH was followed by an increase in phosphorylated form of ERK indicating ERK activation. The increase reached a peak at 8 h after collagenase injection and seemed to have a second peak at 48 h (Fig. 5A). The increase in phosphorylated ERK at 8 h after collagenase injection was largely suppressed when animals were pretreated with argatroban or PD98059 (Fig. 5B).

We also performed immunohistochemical staining of phospho-ERK with NeuN or with OX-42, a microglial marker, to determine which cell type was responsible for elevated levels of phospho-ERK. Both neurons and microglia within the hematoma area exhibited immnoreactivity for phospho-ERK at 8 h after collagenase injection (Fig. 5C-H). Omission of primary antibodies abolished cellular fluorescence staining with secondary antibodies (data not shown), thus confirming specificity of immunopositive signals.

MAP kinase inhibitors induce cell death in microglia

DNA fragmentation as revealed by TUNEL staining occurs in apoptosis and several other forms of cell death, and thrombin induces neuronal nuclear fragmentation in vitro and in vivo (Donovan et al., 1997; Fujimoto et al., 2007). Thus, we next performed TUNEL staining to verify if the neuroprotective effect of PD98059 was associated with suppression of DNA fragmentation. A substantial number of TUNEL-positive cells appeared in the hematoma area at 1 day after collagenase injection. Unexpectedly, PD98059 applied 1 h before collagenase injection did not decrease the number of TUNEL-positive cells (Fig. 6A, B, E and F). Similarly, SB203580 and SP600125 did not inhibit the increase in TUNEL-positive cells in response to ICH (Fig. 6C, D, E and F). Rather, these drugs tended to increase the number

of TUNEL-positive cells in the peripheral region of the hematoma (Fig. 6F).

Then, the types of cells with TUNEL-positive signals were identified by immunohistochemisty against specific marker proteins. In the striatum of animals treated with vehicle (33%DMSO), TUNEL-positive cells in the hematoma area at 1 day after collagenase injection overlapped with NeuN, a neuronal marker, but not with OX-42, a microglial marker (Fig. 7A-F). On the other hand, a substantial number of TUNEL-positive cells showing OX-42 immunoreactivity appeared in the striatum of animals treated with PD98059 (Fig. 7G-I). OX-42-positive cells with TUNEL staining were also observed in animals treated with SB203580 and SP600125 (Fig. 7J-O). These results suggest that inhibition of MAP kinases resulted in induction of cell death in microglia. Therefore, we counted the number of OX-42-positive microglia in the hematoma area at 3 days after collagenase injection. At this time point, microglia were almost exclusively localized at the peripheral region of hematoma, and few microglia were observed at the hematoma center. As shown in Fig. 8, MAP kinase inhibitors tended to decrease the number of microglia in the peripheral region, although the difference between vehicle-treated group and drug-treated groups did not reach statistical significance.

Discussion

The present study was aimed to reveal whether the same cellular mechanisms as those recruited in thrombin-induced neuronal injury were involved in ICH-induced injury in vivo. For this purpose, we examined the effects of argatroban, cycloheximide and several MAP kinase inhibitors on neuronal injury in collagenase-induced ICH model. These drugs have been shown to block thrombin-induced shrinkage of the striatal tissue in organotypic culture (Fujimoto et al., 2006). Here we demonstrated that ICH-induced decrease in the number of surviving neurons in the striatum was significantly prevented by argatroban, cycloheximide and MAP kinase inhibitors. Particularly, neuroprotection by argatroban, a thrombin inhibitor, indicates that exaggerated thrombin activity plays an important role in neuronal injury associated with ICH. Moreover, the effectiveness of cyclohexmide, PD98059 and SP600125 closely parallels the findings in thrombin cytotoxicity on striatal slice culture, and adds further support for the idea that signaling pathways triggered by thrombin are involved in the pathogenesis of ICH.

A notable difference between the results of the present study and those of an in vitro study was that the protective effects of argatroban and cycloheximide in vivo were only partial, whereas these drugs completely blocked striatal shrinkage in slice culture (Fujimoto et al., 2006). Similarly, MAP kinase inhibitors showed only a partial neuroprotective effect in the present study, although they almost completely blocked striatal tissue injury in vitro. A reasonable explanation for these discrepancies is that ICH-induced neuronal injury may involve additional mechanisms independent of thrombin. For example, blood-derived factors other than thrombin, such as hemoglobin and tissue plasminogen activator, may exert harmful influences on central neurons (Huang et al., 2002; Wang et al., 2006). Moreover, mass effect of hematoma (Nehls et al., 1990) and the elevation of intracranial pressure can act as a cause of brain injury. Another possible explanation is that thrombin by itself in the in

vivo context may also recruit MAP kinase-independent mechanisms leading to neuronal death. Indeed, neuronal damage in the striatum induced by direct injection of thrombin was only partially prevented by PD98059, SB203580 and SP600125 (Fujimoto et al., 2007). We also cannot entirely exclude the possibility that the drugs at doses tested were not sufficient to fully counteract with their targets in the signaling pathways.

The extent of hematoma expansion and of edema formation was not significantly altered by any drugs tested in the present study. Consistent with our observations, argatroban has been reported to show no effect on hematoma size (Kitaoka et al., 2002; Nagatsuna et al., 2005), despite the fact that this drug is clinically used for anti-coagulation. On the other hand, the same studies also reported that peripheral administration of argatroban significantly suppressed brain edema associated with ICH (Kitaoka et al., 2002; Nagatsuna et al., 2005), which is discrepant with our results. Although we have no obvious explanations for this discrepancy, many different conditions in experimental settings might affect the consequences. In any case, the results of the present study indicate that neuroprotective effects of drugs including argatroban, cycloheximide and MAP kinase inhibitors against ICH-induced injury are not secondary to amelioration of physically deleterious factors, i.e., hematoma and edema. It should be noted that the types of parameters such as neuron counts, hematoma size and brain water content are different in nature, which might be responsible for their different sensitivities to drug effects.

Activation of ERK after ICH, as revealed by an increase in phosphorylated ERK, was confirmed by western blot analysis. The increase in phosphorylated ERK was largely abolished by treatment with argatroban, suggesting that thrombin plays a major role in activation of ERK following ICH. Phosphorylation of ERK was observed both in neurons and in microglia, which is consistent with the fact that PARs are expressed in both cell types (Noobakhsh et al., 2003). In other words, ERK in both neurons and microglia may have a

potential link to neuronal injury in ICH.

TUNEL staining combined with immunohistochemical identification of cell types indicated that the neuroprotective effects of inhibitors of ERK and other MAP kinases may be in part mediated by inhibition of microglial activities. This conclusion was first led by the observation that MAP kinase inhibitors did not decrease the number of TUNEL-positive cells in the hematoma, while they produced significant neuroprotective effects. This observation was followed by the finding that MAP kinase inhibitors induced TUNEL-positive signals in microglia that were not observed in vehicle-treated animals. Indeed, the number of microglia in the hematoma tended to decrease in animals treated with MAP kinase inhibitors, suggesting that microglial cell death was induced by these treatments. Although microglia have been reported to exert neuroprotective functions under several circumstances such as oxygen-glucose deprivation-induced neuronal damage (Neumann et al., 2006; Schwartz et al., 2006), we have previously shown that microglial activation plays a crucial role in thrombin-induced neuronal injury in the striatum in vitro (Fujimoto et al., 2006). Moreover, partial suppression of microglial activation by a pharmacological treatment significantly inhibited thrombin-induced striatal injury in vivo (Fujimoto et al., 2007). A report by Power et al. (2003) has demonstrated that minocycline is neuroprotective against ICH-induced injury by suppressing microglial activation and downregulating expression of matrix metalloprotease-12. Therefore, arrestment of the increase in microglia by inhibition of MAP kinases may well protect neurons from ICH-induced injury. In this context, MAP kinase signaling pathways have been reported to mediate proliferation of microglia induced by corticotropin-releasing hormone (Wang et al., 2003). On the other hand, many lines of evidence have shown that activation of neuronal MAP kinases is deleterious to neurons. For example, ERK activation leads to cell death of rat cerebellar granule neurons through plasma membrane damage (Subramaniam et al., 2004). Relative contribution of neuronal and

microglial MAP kinases to ICH-induced neuronal injury should be addressed in detail in further investigations.

In conclusion, we have shown that signaling mechanisms triggered by blood-derived thrombin, including MAP kinases, have an important role in ICH-induced neuronal injury. We also suggest that one of the roles of activated MAP kinases is to support the survival of microglia in the hematomal region, thereby assuring cytotoxic activities of microglia onto neurons. Regulation of MAP kinases and micoglial activities should be an important strategy to prevent the progression of pathogenic events associated with ICH. From a clinical point of view, effectiveness of drugs that inhibit thrombin, MAP kinases and microglial activities against ICH-induced injury should be investigated in further detail, including dosing regimens based solely on post-insult treatments.

Acknowledgements

This study was supported by Grant-in-aid for Scientific Research from The Ministry of Education, Culture, Sports, Science and Technology, Japan and Japan Society for the Promotion of Science. S. F. was supported as a Research Assistant by 21st Century COE Program “Knowledge Information Infrastructure for Genome Science”.

References

Donovan, F.M., Pike, C.J., Cotman, C.W., Cunningham, D.D. 1997. Thrombin induces apoptosis in cultured neurons and astrocytes via a pathway requiring tyrosine kinase and RhoA activities. J. Neurosci. 17, 5316-5326.

Donovan, F.M., Cunningham, D.D., 1998. Signaling pathways involved in thrombin-induced cell protection. J. Biol. Chem. 273, 12746-12752.

Fayad, P.B., Awad, I.A. 1998. Surgery for intracerebral hemorrhage. Neurology **51:** S69-73.

Flynn, A.N. and Buret, A.G. 2004. Proteinase-activated receptor 1 (PAR-1) and cell apoptosis. Apoptosis 9, 729-737.

Fujimoto, S., Katsuki, H., Ohnishi, M., Takagi, M., Kume, T., Akaike, A. 2007. Thrombin induces striatal neurotoxicity depending on mitogen-activated protein kinase pathways in vivo. Neuroscience 144, 694-701.

Fujimoto, S., Katsuki, H., Kume, T., Akaike, A. 2006. Thrombin-induced delayed injury involves multiple and distinct signaling pathways in the cerebral cortex and the striatum in organotypic slice cultures. Neurobiol. Dis. 22, 130-142.

Hua, Y., Schallert, T., Keep, R. F., Wu, J., Hoff, J. T., Xi, G. 2002. Behavioral tests after intracerebral hemorrhage in the rat. Stroke 33, 2478-2484.

Huang, F.P., Xi, G., Keep, R. F., Hua, Y., Nemoianu, A., Hoff, J. T. 2002. Brain edema after experimental intracerebral hemorrhage: role of hemoglobin degradation products. J Neurosurg. 96, 287-293.

Kitaoka, T., Hua, Y., Xi, G., Hoff, J.T., Keep, R.F. 2002. Delayed argatroban treatment reduces edema in a rat model of intracerebral hemorrhage. Stroke 33, 3012-3018.

Marinissen, M.J., Servitja, J.M., Offermanns, S., Simon, M.I., Gutkind, J.S. 2003. Thrombin protease-activated receptor-1 signals through Gq- and G_{13}-initiated MAPK cascades regulating c-Jun expression to induce cell transformation. J. Biol. Chem. 278, 46814-46825.

Nagatsuna, T., Nomura, S., Suehiro, E., Fujisawa, H., Koizumi, H., Suzuki, M. 2005. Systemic administration of argatroban reduces secondary brain damage in a rat model of intracerebral hemorrhage: Histopathological assessment. Cerebrovasc. Dis. 19, 192-200

Nehls, D.G., Mendelow, D.A., Graham, D.I., Teasdale, G.M. 1990. Experimental intracerebral hemorrhage: early removal of a spontaneous mass lesion improves late outcome. Neurosurgery 27, 674-682.

Neumann, J., Gunzer, M., Gutzeit, H.O., Ullrich, O., Reymann, K.G., Dinkel, K. 2006. Microglia provide neuroprotective after ischemia. FASEB J. 20, 714-716.

Noorbakhsh, F., Vergnolle, N., Hollenberg, M.D., Power, C. 2003. Proteinase-activated receptors in the nervous system. Nat. Rev. Neurosci. 4, 981-990.

Power, C., Henry, S., Del Bigio, M.R., Larsen, P.H., Corbett, D., Imai, Y., Yong, V.W., Peeling, J. 2003. Intracerebral hemorrhage induces macrophage activation and matrix metalloproteinases. Ann Neurol. 53, 731-742.

Schwartz, M., Butovsky, O., Bruck, W., Hanisch, U.K., 2006. Microglial phenotype: is the commitment reversible? Trends Neurosci. 29, 68-74.

Striggow, F., Riek, M., Breder, J., Henrich-Noack, P., Reymann, K.G., Reiser, G., 2000. The protease thrombin is an endogenous mediator of hippocampal neuroprotection against ischemia at low concentrations but causes degeneration at high consentrations. Proc. Natl. Acad. Sci. USA. 97, 2264-2269.

Subramaniam, S., Zirrgiebel, U., von Bohlen und Halbach, O., Strelau, J., Laliberté, C., Kaplan, D. R., Unsicker, K. 2004. ERK activation promotes neuronal degeneration predominantly through plasma membrane damage and independently of caspase-3. J. Cell Biol. 165, 357-369.

Suo, Z., Wu, M., Citron, B. A., Palazzo, R.E., Festoff, B.W. 2003. Rapid tau aggregation and delayed hippocampal neuronal death induced by persistent thrombin signaling. J. Biol. Chem.

278, 37681-37689.

Terai, K., Suzuki, M., Sasamata, M., Miyata, K. 2003. Amount of bleeding and hematoma size in the collagenase-induced intracerebral hemorrhage rat model. Neurochem. Res. 28, 779-785.

Vaughan, P.J., Pike, C.J., Cotman, C.W., Cunningham, D.D., 1995. Thrombin receptor activation protects neurons and astrocytes from cell death produced by environmental insults. J. Neurosci. 15, 5389-5401.

Wang, H., Ubl, J.J., Stricker, R., Reiser, G. 2002. Thrombin (PAR-1)-induced proliferation in astrocytes via MAPK involves multiple signaling pathways. Am. J. Physiol. Cell Physiol. 283, C1351-1364.

Wang, S., Lee, S. R., Guo, S. Z., Kim, W., J., Montaner, J., Wang, X., Lo, E. H. 2006. Reduction of tissue plasminogen activater-induced matrix metalloproteinase-9 by simvastatin in astrocytes. Stroke 37, 1910-1912.

Wang, W., Ji, P., Dow, K. E. Corticotropin-releasing hormone induces proliferation and TNF-α release in cultured rat microglia via MAP kinase signalling pathways. 2003. J. Neurochem. 84, 189-195

Xi, G., Keep, R.F., Hoff, J.T. 2006. Mechanisms of brain injury after intracerebral hemorrhage. Lancet Neurol. 5, 53-63.

Xue, M., Del Bigio, M. R. 2003. Comparison of brain cell death and inflammatory reaction in three models of intracerebral hemorrhage in adult rats. J. Stroke Cerebrovas. Dis. 12, 152-159.

Figure legends

Fig. 1 Representative images of NeuN-immunostained coronal sections obtained 3 days after sham treatment (saline injection; A and C) or collagenase injection (ICH; B and D). At low magnification (A and B), a decrease in NeuN immunoreactivity was evident at hematoma region in ICH group. Magnified views (C and D) reveal a substantial decrease in the number of NeuN-positive cells in the center of hematoma. Asterisk indicates the peripheral region of hematoma.

Fig. 2 Effects of argatroban and cycloheximide on ICH-induced neuronal damage. (A-D) Shown are representative images of NeuN-immunostained coronal sections obtained 3 days after intrastriatal injection of saline (Sal; A) or collagenase (Col; B-D). The animals also received intracerebroventricular injections of saline (A and B), argatroban (ARG; C) or cycloheximide (CHX; D). Scale bar = 50 μm. (E, F) The number of NeuN-positive cells at the center (E) and the peripheral region (F) of hematoma. n = 5-10 for each condition. *** $P < 0.001$ vs. sham group; # $P < 0.05$ vs. col + sal group. Data in panel F were analyzed with Kruskal-Wallis test followed by Dunn's multiple comparisons test.

Fig. 3 Involvement of MAP kinases in ICH-induced neuronal damage. (A-E) Representative images of NeuN-immunostained coronal sections obtained 3 days after intrastriatal injection of saline (Sal; A) or collagenase (Col; B-E) are shown. The animals also received intracerebroventricular injections of vehicle (33% DMSO; A and B), PD98059 (PD; C), SB203580 (SB; D) or SP600125 (SP; E). Scale bar = 50 μm. (F, G) The number of NeuN-positive cells at the center (F) and the peripheral region (G) of hematoma. n = 5-8 for each condition. *** $P < 0.001$ vs. sham group; # $P < 0.05$, ## $P < 0.01$ vs. col + DMSO group. Data in panel F were analyzed with Kruskal-Wallis test followed by Dunn's multiple

comparisons test.

Fig. 4 Brain water content at 3 days after intrastriatal injection of saline (Sal) or collagenase (Col). The upper panel shows the effects of argatroban (ARG) and cycloheximide (CHX), and the lower panel shows the effects of PD98059 (PD), SB203580 (SB) and SP600125 (SP). These drugs were administered into lateral ventricle. Slice A includes the site of intrastriatal injection, and the adjacent caudal slice was designated as B. ICH induced a significant increase in brain water content, which was not affected by any drugs tested. n = 4-5 for each condition. ** $P < 0.01$, *** $P < 0.001$; N.S., not significant.

Fig. 5 Activation of ERK in response to ICH. (A) Phosphorylation of ERK at indicated time points after intrastriatal injection of saline or collagenase. (B) Effects of argatroban (ARG) and PD98059 (PD) on ERK phosphorylation were determined at 8 h after intrastriatal injection of saline or collagenase. Saline (Sal), ARG and PD were administered into lateral ventricle 1 h before intrastriatal injection of saline or collagenase. Panels A and B are representative images, each from 5 independent sets of experiments. (C-H) Immunohistochemistry of phosphorylated ERK (p-ERK) with NeuN (C-E) or with OX-42 (F-H) on sections obtained at 8 h after collagenase injection. Arrows in merged images (E and H) indicate co-localization of immunopositive signals. Scale bar = 20 μm.

Fig. 6 Effects of MAP kinase inhibitors on the number of TUNEL-positive cells appearing after ICH. (A-D) Representative TUNEL images of the peripheral region of hematoma in coronal sections obtained 1 day after intrastriatal injection of collagenase. The animals also received intracerebroventricular injections of vehicle (33% DMSO; A), PD98059 (PD; B), SB203580 (SB; C) or SP600125 (SP; D). Scale bar = 50 μm. (E, F) The number of

TUNEL-positive cells at the center (E) and the peripheral region (F) of hematoma at 1 day after collagenase injection. n = 6-7 for each condition.

Fig. 7 Identification of TUNEL-positive cells. TUNEL with immunohistochemistry was done on brain sections obtained 1 day after collagenase injection. Animals also received intracerebroventricular injection of vehicle (DMSO), PD98059 (PD), SB203580 (SB) or SP600125 (SP) 1 h before collagenase injection. In vehicle-treated animals, TUNEL staining colocalized with NeuN immunoreactivity (A-C) but not with OX-42 immunoreactivity (D-F). In contrast, substantial colocalization of TUNEL staining with OX-42 immunoreactivity, indicated by arrows, was observed in animals treated with PD (G-I), SB (J-L) and SP (M-O). Scale bar = 20 μm.

Fig. 8 Effects of MAP kinase inhibitors on the number of microglia in the peripheral region of hematoma. (A-D) OX-42 immunohistochemistry was done on brain sections obtained 3 days after collagenase injection. Animals also received intracerebroventricular injection of vehicle (DMSO; A), PD98059 (PD; B), SB203580 (SB; C) or SP600125 (SP; D). Scale bar = 50 μm. (E) The number of microglia in the peripheral region of hematoma at 3 days after collagenase injection. n = 7-8 for each condition.

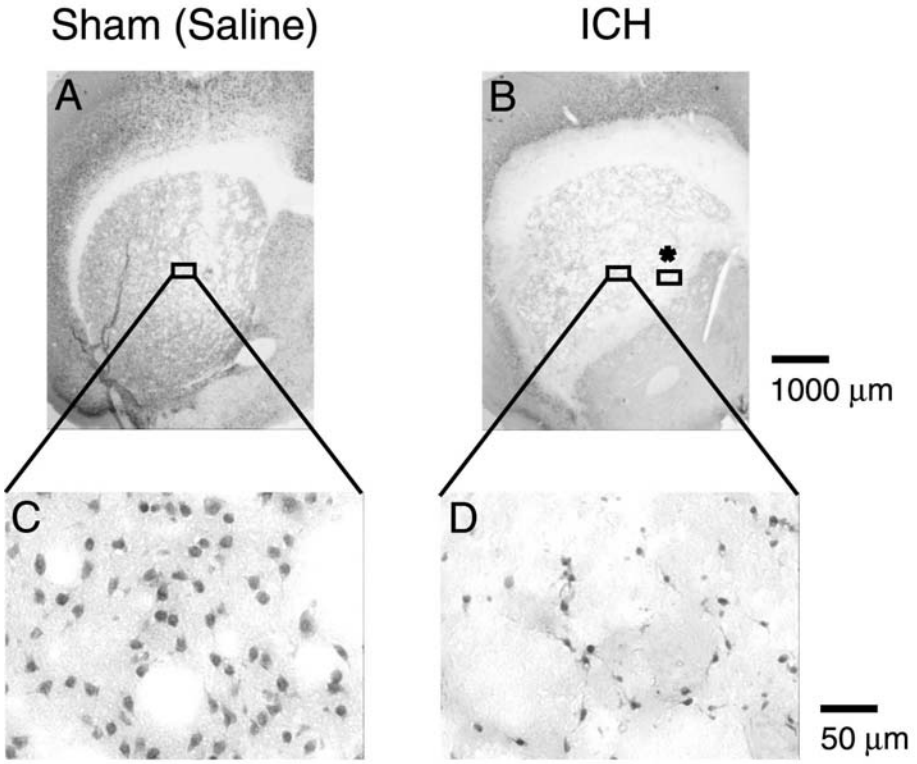
Sham (Saline)
ICH
A
B
1000 μm
C
D
50 μm

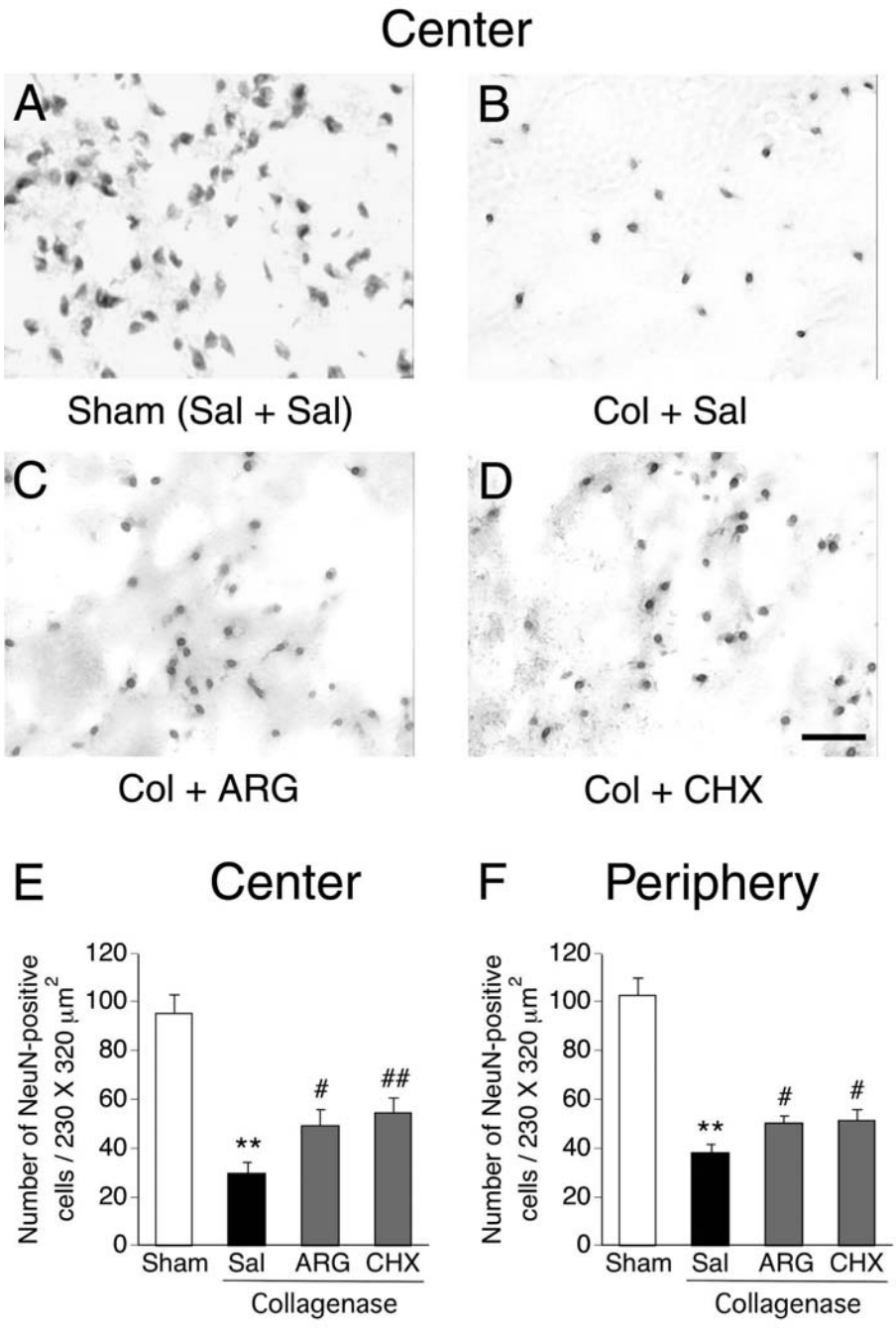
Center
A
B
Sham (Sal + Sal)
Col + Sal
C
D
Col + ARG
Col + CHX
E
Center
F
Periphery
Number of NeuN-positive cells / 230 X 320 μm2
120
100
80
60
40
20
0
**
#
##
Sham
Sal
ARG
CHX
Collagenase

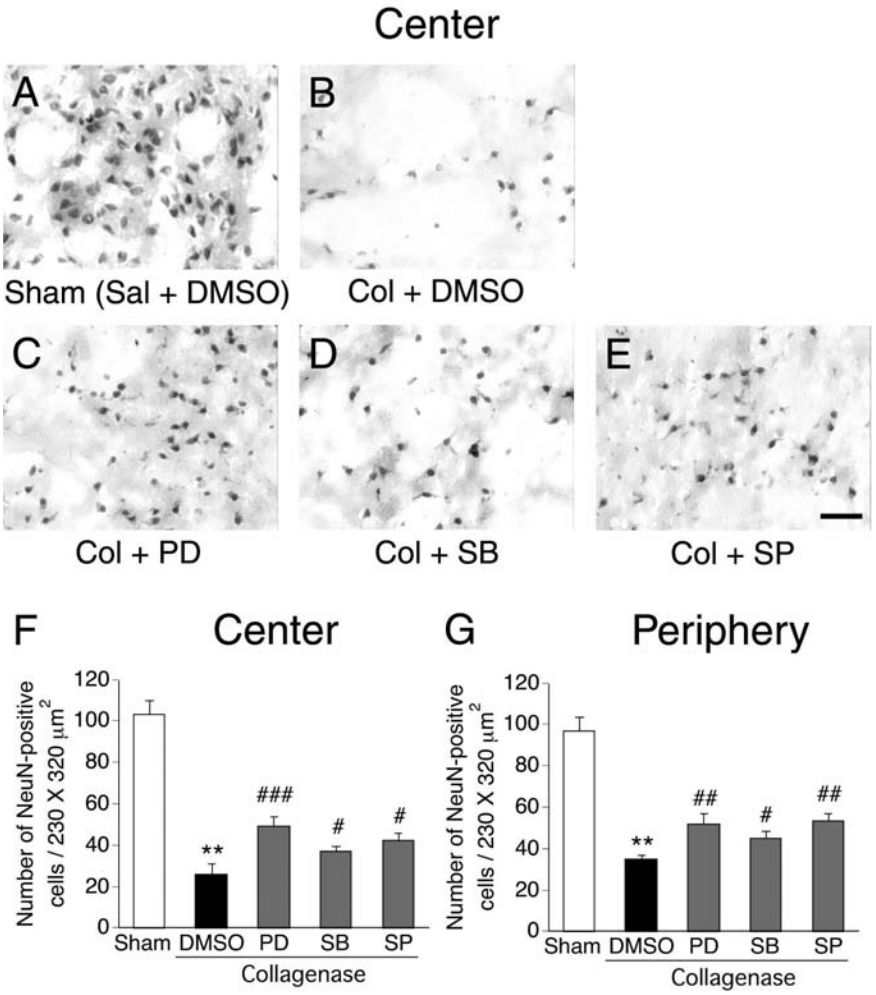
Center
A
B
Sham (Sal + DMSO)
Col + DMSO
C
D
E
Col + PD
Col + SB
Col + SP
F
Center
G
Periphery
Number of NeuN-positive cells / 230 X 320 μm2
120
100
80
60
40
20
0
**
###
#
#
##
Sham
DMSO
PD
SB
SP
Collagenase

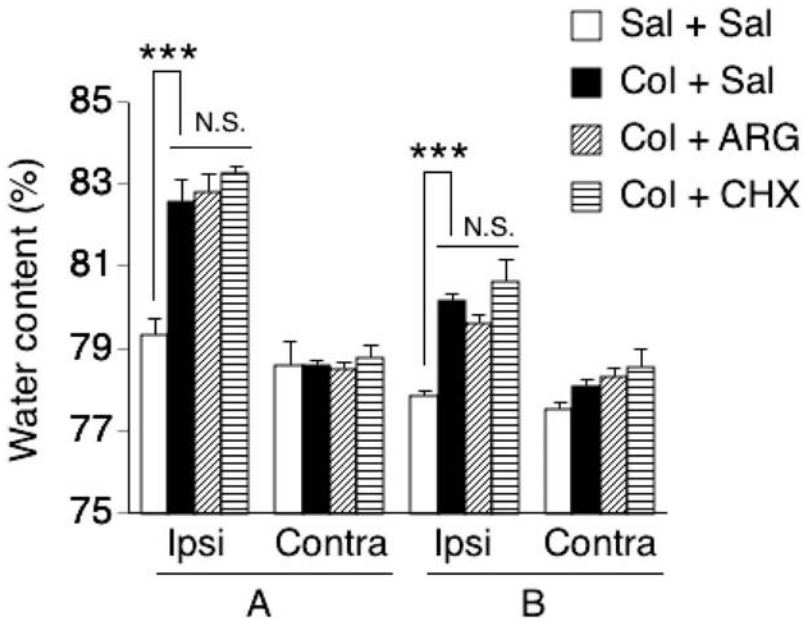
Sal + Sal
Col + Sal
Col + ARG
Col + CHX
Water content (%)
85
83
81
79
77
75
***
N.S.
***
N.S.
Ipsi
Contra
Ipsi
Contra
A
B

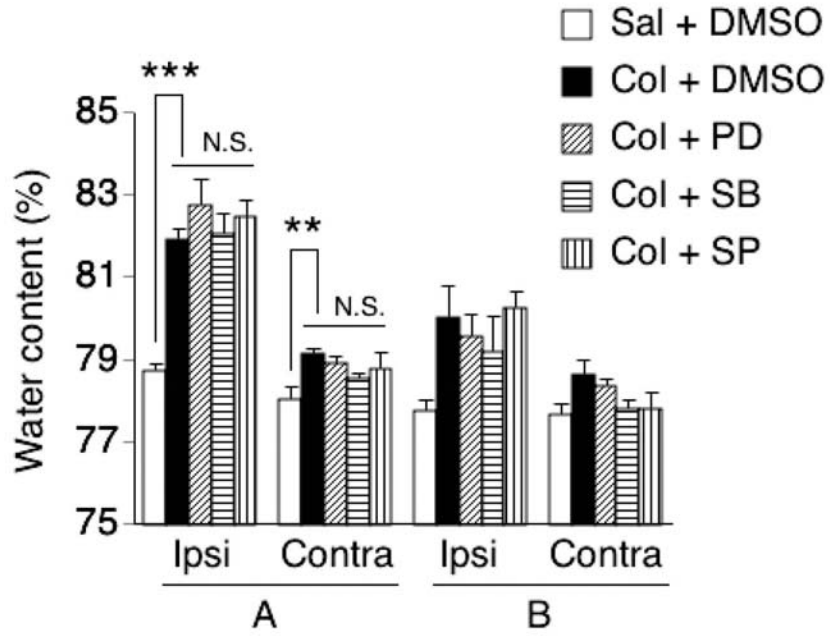
Sal + DMSO
Col + DMSO
Col + PD
Col + SB
Col + SP
Water content (%)
85
83
81
79
77
75
***
N.S.
**
N.S.
Ipsi
Contra
Ipsi
Contra
A
B

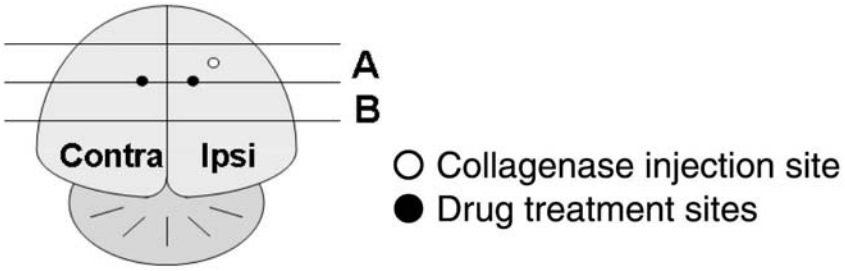
A
B
Contra
Ipsi
Collagenase injection site
Drug treatment sites

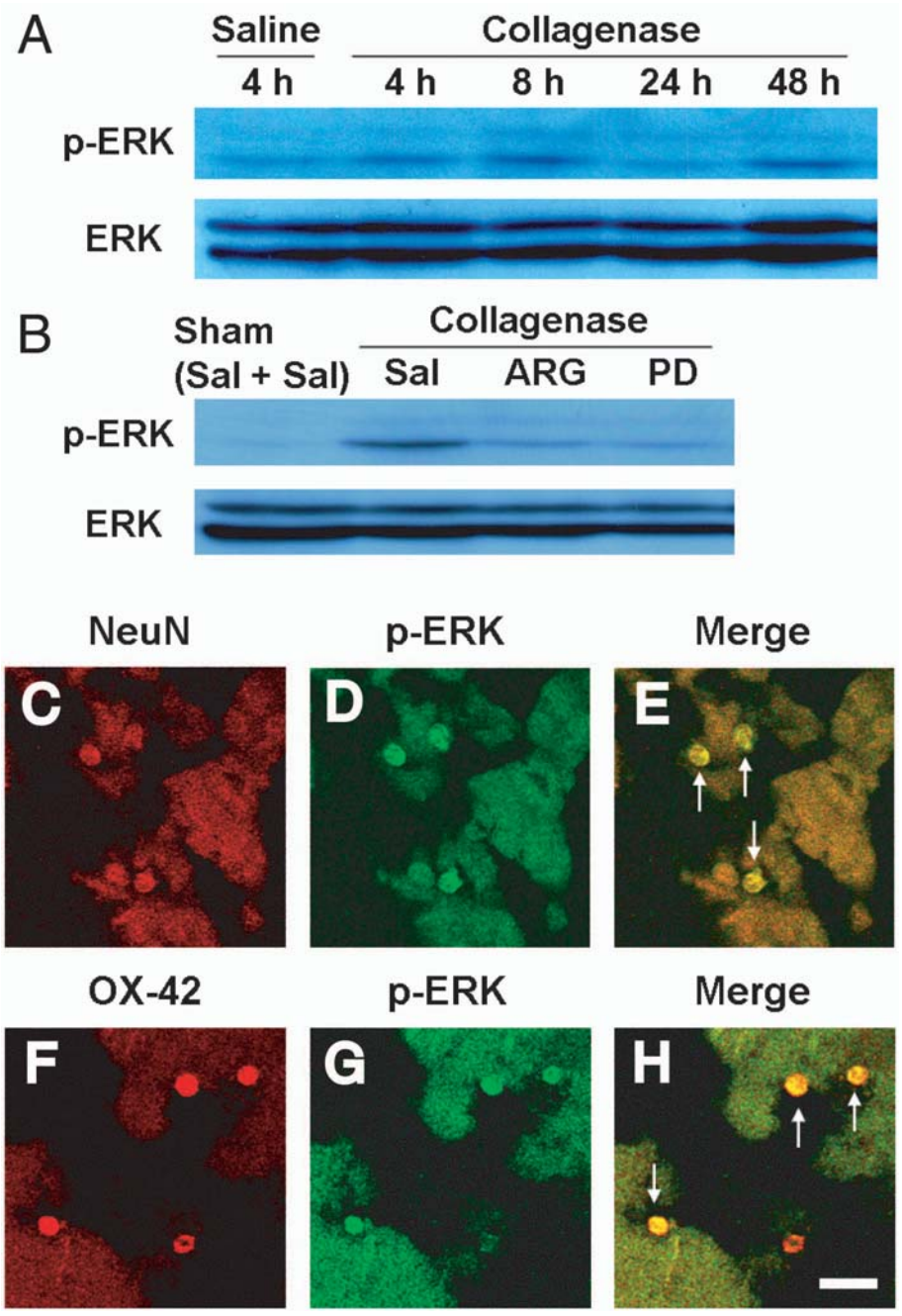
A
Saline
Collagenase
4 h
4 h
8 h
24 h
48 h
p-ERK
ERK
B
Sham
(Sal + Sal)
Collagenase
Sal
ARG
PD
p-ERK
ERK
NeuN
p-ERK
Merge
C
D
E
OX-42
p-ERK
Merge
F
G
H

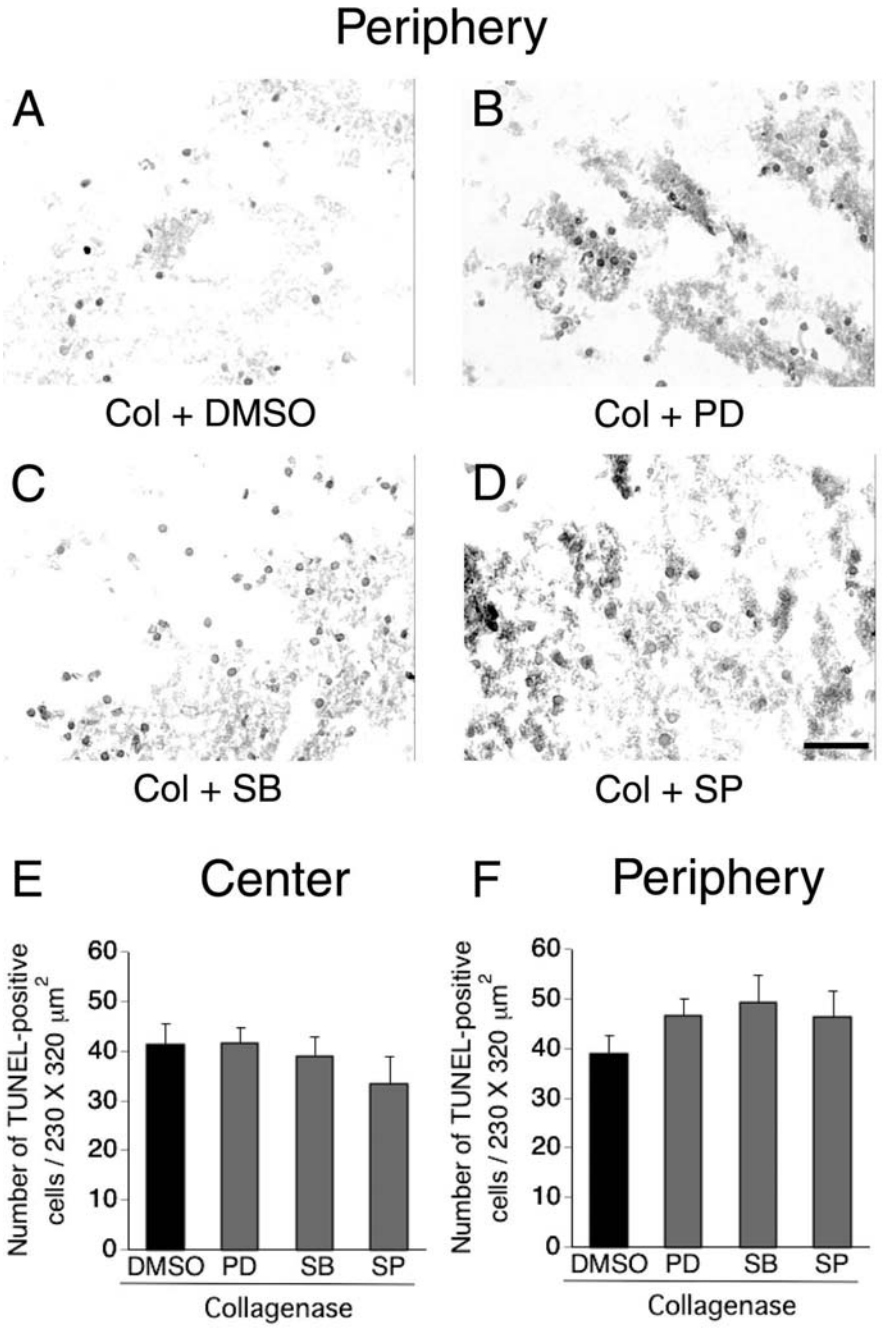
Periphery
A
B
Col + DMSO
Col + PD
C
D
Col + SB
Col + SP
E
Center
F
Periphery
Number of TUNEL-positive cells / 230 X 320 μm2
60
50
40
30
20
10
0
DMSO
PD
SB
SP
Collagenase

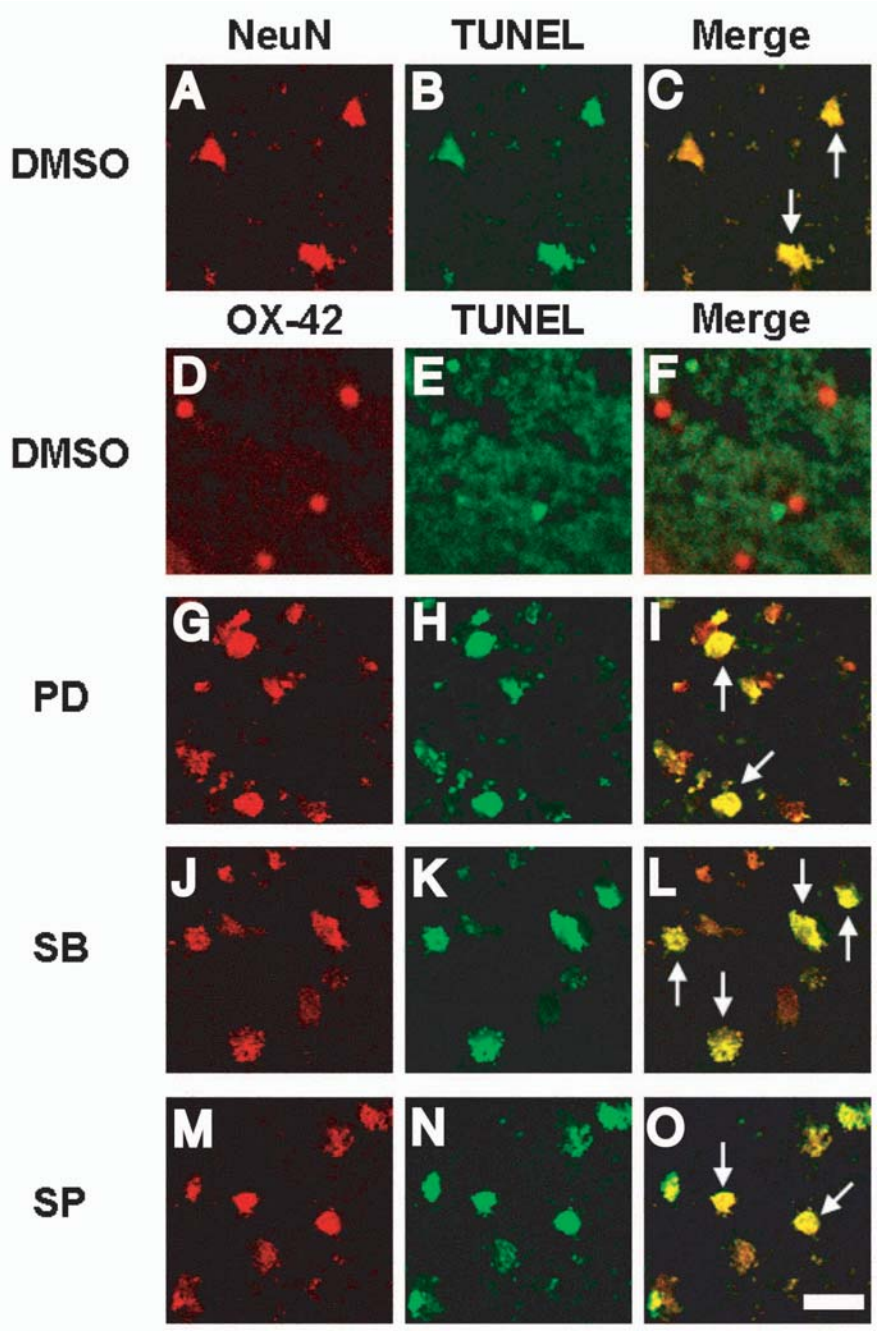
NeuN
TUNEL
Merge
DMSO
A
B
C
OX-42
TUNEL
Merge
DMSO
D
E
F
PD
G
H
I
SB
J
K
L
SP
M
N
O

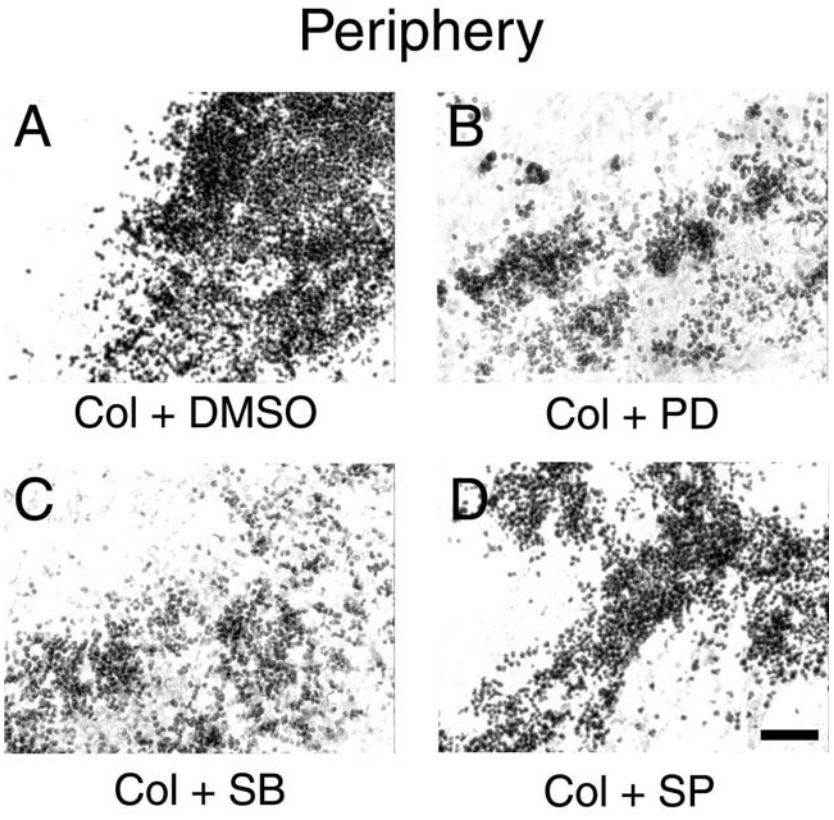
Periphery
A
B
Col + DMSO
Col + PD
C
D
Col + SB
Col + SP

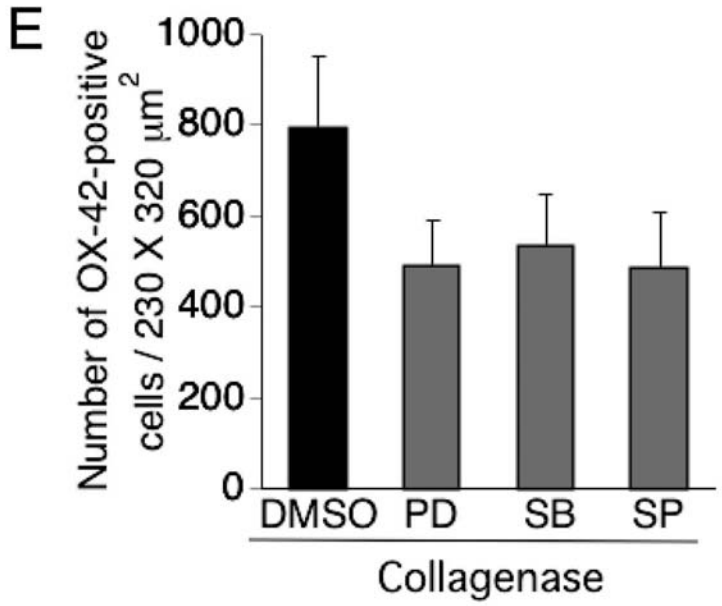
E
Number of OX-42-positive cells / 230 X 320 μm2
1000
800
600
400
200
0
DMSO
PD
SB
SP
Collagenase